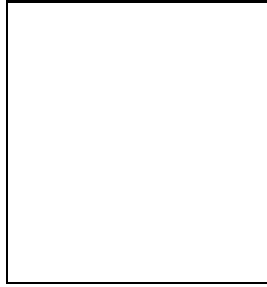


# GAMMA-RAY PRODUCTION IN SUPERNOVA REMNANTS

Matthew G. BARING<sup>a</sup>

*Laboratory for High Energy Astrophysics, Code 661,  
NASA/Goddard Space Flight Center, Greenbelt, MD 20771, U.S.A.*



Supernova remnants are widely believed to be a principal source of galactic cosmic rays, produced by diffusive shock acceleration in the environs of the remnant's expanding shock. This review discusses recent modelling of how such energetic particles can produce gamma-rays via interactions with the remnants' ambient interstellar medium, specifically via neutral pion decay, bremsstrahlung and inverse Compton emission. Predictions that relate to the handful of associations between EGRET unidentified sources and known radio/optical/X-ray emitting remnants are summarized. The cessation of acceleration above 1 TeV - 10 TeV energies in young shell-type remnants is critical to model consistency with Whipple's TeV upper limits; these observations provide important diagnostics for theoretical models.

## 1 Introduction

For many years now it has been a common perception that supernova remnants (SNRs) are a principal, if not the predominant, source of galactic cosmic rays (e.g. see Lagage and Cesarsky<sup>1</sup>) up to energies of around  $\sim 10^{15}$  eV, where the so-called *knee* in the spectrum marks its deviation from almost pure power-law behaviour (e.g. see Hillas<sup>2</sup> for a depiction of the spectrum). Such cosmic rays are presumed to be produced by diffusive shock (Fermi) acceleration in the environs of the shock that is initiated by the impact of the supernova ejecta on the surrounding interstellar medium. The convenience of a SNR origin of cosmic rays below the knee is founded in (i) the appropriateness of their ages (between 100 and  $10^5$  years) and sizes for permitting the diffusive process to accelerate up to such high energies (see below and the discussion in ref. [1]), (ii) they have the necessary power to amply satisfy cosmic ray energetics requirements, and (iii) that current estimates of supernova rates in our galaxy can adequately supply the observed cosmic ray density (e.g. see the review of Blandford and Eichler<sup>3</sup>).

---

<sup>a</sup>Compton Fellow, USRA. Email: [Baring@lheavx.gsfc.nasa.gov](mailto:Baring@lheavx.gsfc.nasa.gov)

The evidence for cosmic ray acceleration in remnants is, of course, circumstantial. Nevertheless, the ubiquity of polarized, non-thermal radio emission in remnants (e.g. see references in the SNR compendium of Green<sup>4</sup>) argues convincingly for efficient acceleration of electrons if the synchrotron mechanism is assumed responsible for the emission. X-rays also abound in remnants, and are usually attributed to thermal emission from shock-heated electrons (because of the appearance of spectral lines, e.g. see Borkowski et al.<sup>5</sup> for Cas A; see also the review of Ellison et al.<sup>6</sup>). The striking spatial coincidence of radio and X-ray images of remnants (e.g. Tycho<sup>3</sup> and SN1006; see Keohane et al.<sup>7</sup> for a radio/X-ray correlation analysis for Cas A) suggests that the same mechanism is responsible for emission in both wavebands. This contention has recently received a major boost with the discovery of non-thermal X-ray emission in SN1006 by Koyama et al.<sup>8</sup>, which implies the presence of non-thermal electrons at super TeV energies (see Reynolds<sup>9</sup> for a detailed description). In addition, very recent ASCA spectra (Keohane et al.<sup>10</sup>) for the remnant IC 443 and RXTE observations of Cas A (Allen et al.<sup>11</sup>) exhibit non-thermal X-ray contributions, adding to the collection of TeV electron-accelerators. A nice review of radio and X-ray properties of SNRs is given in Ellison et al.<sup>6</sup>.

An offshoot of cosmic ray acceleration in SNRs is that such energetic particles can produce gamma-rays via interactions with the ambient interstellar medium (ISM). Although no unequivocal evidence for gamma-ray emission from isolated supernova remnants exists, Esposito et al.<sup>12</sup> presents a handful of associations between unidentified EGRET sources (at above 100 MeV) in or near the galactic plane and known radio/optical/X-ray-emitting (relatively young) remnants, providing ample motivation for exploring the possibility of high energy emission from SNRs. Such associations are suggestive<sup>13</sup>, but suffer from the large uncertainty<sup>12</sup> in position location of EGRET sources, of the order of 0.5–1 degrees, i.e. the size of typical nearby remnants (see the images depicted in Figure 1). Hence a definitive connection between *any* of these gamma-ray sources and the young SNRs is not yet possible. The situation is complicated by the presence of a pulsar (PSR B1853+01) in the field<sup>12,14</sup> of the 95% confidence contour of the EGRET source 2EG J1857+0118. Such a pulsar (or its wind nebula) could easily spawn the observed gamma-ray emission (which has so far yielded no evidence of pulsation<sup>15</sup>), and the conceivability that pulsars could be responsible for most unidentified EGRET sources near the galactic plane<sup>16</sup> (discussed in the review by Grenier in this volume) currently inhibits any assertions stronger than just suggestions of a remnant/EGRET source connection.

In this paper, the handful of SNR gamma-ray emission models that invoke shock acceleration and have been developed in the last four years are reviewed. This field began in earnest (following limited early work<sup>17,18</sup>) with the seminal paper of Drury, Aharonian and Völk<sup>19</sup>, who computed the photon spectra expected from the decay of neutral pions generated in collisions between shock-accelerated ions and cold ions in the ISM. Their work used a two-fluid approach to shock acceleration. Since, then there has been a small flurry of activity, with different groups using alternative approaches, and extending the considerations to include bremsstrahlung and inverse Compton emission. Following a brief summary of supernova remnant expansion properties that are relevant to the acceleration and ultimate energies of cosmic rays, the various models of gamma-ray production will be discussed. Then the focus will turn to very recent work on the relevance of non-linear effects in shock acceleration theory (discussed in the review paper of Baring<sup>20</sup> in this volume) to the SNR  $\gamma$ -ray spectra. These effects describe the dynamical influence of the accelerated cosmic rays on the shocked plasma at the same time as the non-uniformities in the fluid flow force the distribution of the cosmic rays to deviate from pure power-laws. The recent TeV upper limits obtained<sup>21</sup> by the Whipple air Čerenkov detector (discussed by Weekes, this volume) play a very significant role in SNR  $\gamma$ -ray models; contrary to common perception, the various models can be comfortably fine-tuned to accommodate this observational data. Finally, recent work on broad-band approaches to SN1006 and W44 is addressed, indicating the myriad of possibilities for potential  $\gamma$ -ray-emitting supernova remnants.

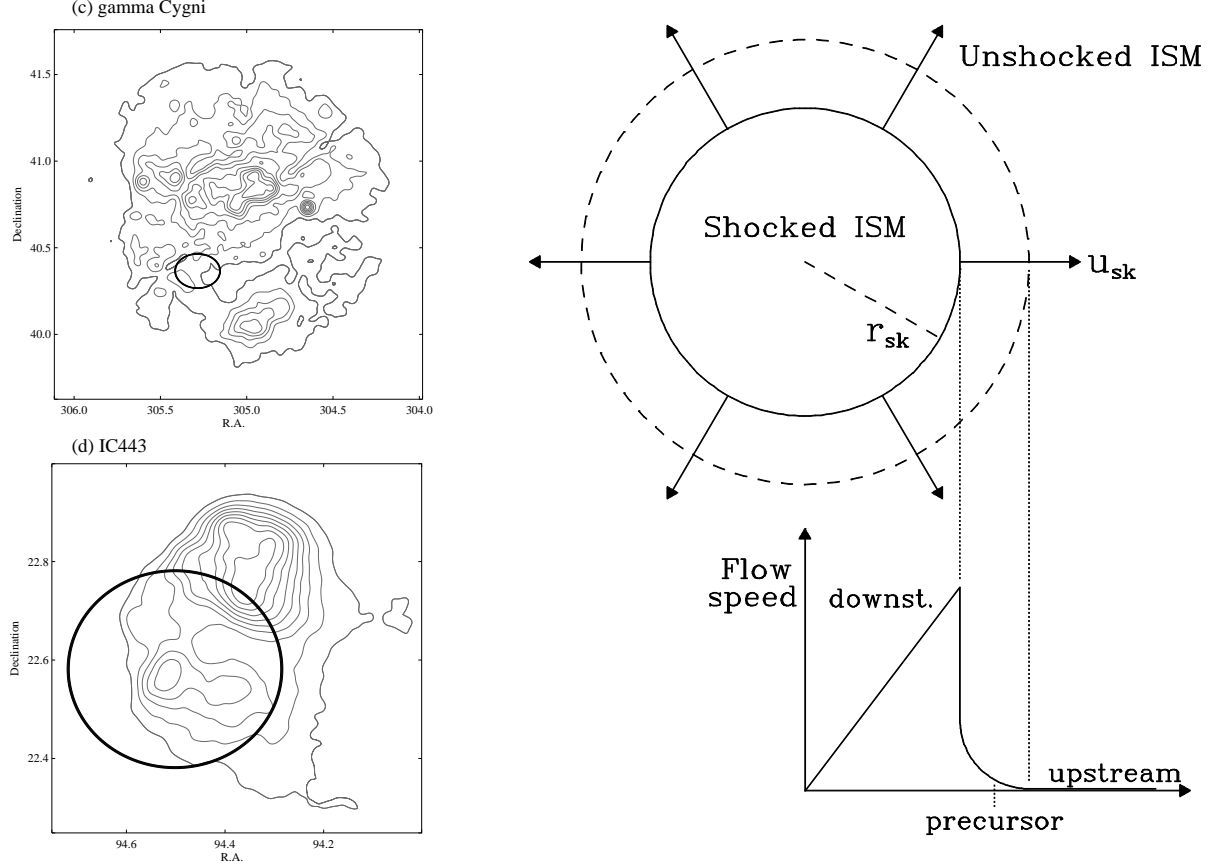


Figure 1: On the left are X-ray/gamma-ray images of the supernova remnants  $\gamma$  Cygni and IC443, as presented in Esposito et al.<sup>12</sup>. These consist of X-ray contours from the ROSAT telescope’s HRI, and the 95% confidence contours of emission above 100 MeV in associated EGRET unidentified sources. On the right is a schematic depiction of an expanding supernova remnant (in the Sedov phase) together with its flow velocity spatial profile in the observer’s frame (downstream material with higher speeds is to the left of the shock discontinuity).

## 2 Supernova Remnant Expansions

It is instructive to review briefly the current conception of a relatively young supernova remnant expansion. This age, which is broadly categorized as being between around 100 years and several thousand years, is appropriate to  $\gamma$ -ray emission models for the five EGRET source associations listed in Esposito et al.<sup>12</sup>. The low end of this range defines the termination of the epoch of approximately free expansion and the gradual onset of the *Sedov* (or scaling) phase of remnant evolution, during which the remnant decelerates as it sweeps up the surrounding interstellar medium. During its expansion, the remnant has a propagating forward shock initiated by the slamming of the supernova ejecta into the ISM outside, producing an adiabatically-expanding interior composed of shocked ISM (see Figure 1 for a depiction). It is during the Sedov phase that this shock is most efficient at depositing its energy into cosmic rays with subsequent conversion to  $\gamma$ -rays: Drury et al.<sup>19</sup> found that the  $\gamma$ -ray emissivity indeed peaks during this part of the SNR evolution. At late stages, the Sedov phase has weakened the shock considerably, and eventually it becomes radiative after tens of thousands of years, i.e. in the post-gamma-ray epoch.

The standard Sedov solution (e.g. Lang<sup>22</sup>) for an explosion of initial energy  $E_{\text{SN}}$ , in a gas of density  $\rho = 1.4n_1m_p$  for number density  $n_1$  (the 1.4 factor accounts for the cosmic abundance of helium and heavier elements) is

$$u_{\text{sk}} = \frac{2}{5}\xi\left(\frac{E_{\text{SN}}}{\rho}\right)^{1/5}t_{\text{SNR}}^{-3/5}, \quad r_{\text{sk}} = \xi\left(\frac{E_{\text{SN}}}{\rho}\right)^{1/5}t_{\text{SNR}}^{2/5}, \quad (1)$$

for the shock speed  $u_{\text{sk}}$  and radius  $r_{\text{sk}}$ , as a function of the SNR age,  $t_{\text{SNR}}$ . Here  $\xi \approx 1.15$ . The onset of the Sedov phase occurs smoothly over a range of times about some time  $t_{\text{Sed}}$ , which is defined roughly by when the mass of the supernova ejecta becomes comparable to that of the ISM it displaces i.e. when  $u_{\text{sk}}$  equals the free-expansion speed  $\sqrt{2E_{\text{SN}}/M_{\text{ej}}}$ . This yields  $t_{\text{Sed}} \sim 0.1E_{\text{SN}}^{-1/2} M_{\text{ej}}^{5/6} (n_1 m_p)^{-1/3}$ , and therefore values of 50 to 300 years for  $E_{\text{SN}} \sim 10^{51}$  ergs. During the Sedov phase, the shock speed is typically 200–3,000 km/sec.

A property of Fermi acceleration that is crucial to the interpretation of spectra via theoretical models is the maximum energy of cosmic rays permitted in a remnant at its present age. Obviously, since the first-order Fermi process involves monotonic evolution of energies with time, the acceleration time to a given energy cannot exceed the age of the remnant. Thereby, one bound to the maximum energy can be obtained. From standard particle diffusion theory, the oft-quoted form for the acceleration time  $\tau_a$ , to a given energy  $E_{\text{max}}$  was derived by Forman and Morfil<sup>23</sup>. Their formula is applied here to plane-parallel shocks, but can be easily adapted to shocks of arbitrary obliquity<sup>24,25</sup>. For  $r = u_1/u_2$ , their result gives an acceleration time

$$\tau_a \sim 10^4 \frac{r(1+r)}{r-1} \frac{\eta}{Q} \left( \frac{B_1}{3\mu\text{G}} \right)^{-1} \left( \frac{E_{\text{max}}}{10^2 \text{TeV}} \right) \left( \frac{u_{\text{sk}}}{10^3 \text{km s}^{-1}} \right)^{-2} \text{years.} \quad (2)$$

Equating this to  $t_{\text{SNR}}$  gives an upper limit to the maximum energy of acceleration  $E_{\text{max}}$ . Acceleration is also limited in the spatial domain: the typical diffusion scale  $d_{\text{diff}} \sim \kappa_{\text{max}}/u_{\text{sk}} = \eta r_{\text{g,max}} c / (3u_{\text{sk}}) = \eta E_{\text{max}} / (3eQ u_{\text{sk}} B_1)$  must be somewhat less than the current remnant size  $r_{\text{sk}}$ , due to escape upstream of the shock in a spherical geometry. Here  $\eta = \lambda/r_g$  for mean free paths  $\lambda$ . The relevant size of the acceleration region can further be constrained by the presence of dense neutral regions or incompletely ionized media<sup>26</sup> in the environs of the shock, since such regions strongly suppress wave generation, and therefore also the Fermi process. For young SNRs early in the Sedov epoch,  $d_{\text{diff}} \lesssim 0.1r_{\text{sk}}$ , a result that is in accord with the non-linear analysis of Drury et al.<sup>19</sup> (see below), and the derived spatial/temporal limit on  $E_{\text{max}}$  is

$$E_{\text{max}} \sim 0.1 \frac{Q}{\eta} \left( \frac{B_1}{3\mu\text{G}} \right) \left( \frac{u_{\text{sk}}}{10^3 \text{km s}^{-1}} \right)^2 \left( \frac{t_{\text{SNR}}}{10^3 \text{yr}} \right) \text{TeV.} \quad (3)$$

This generally yields  $E_{\text{max}}$  (which peaks in the Sedov phase) for ions that are in the 1–30 TeV range per nucleon, depending on the remnant parameters. Note that effects of shock obliquity can act to increase the maximum energy<sup>24</sup>, which becomes crucial to easing constraints<sup>9</sup> imposed by the observations of non-thermal X-rays in SN1006. As discussed in Baring<sup>20</sup>, effecting such increases in  $E_{\text{max}}$  compromises the efficiency of generating populations at these high energies.

### 3 Gamma-Ray Production Models

In the generation of gamma-rays in SNR environments, there are a handful of processes that are relevant, spawned by the collisions of shock-accelerated electrons and ions with the cold ISM. Foremost among these is the decay of neutral pions, which are formed in hadronic collisions  $pp \rightarrow p\pi^0 X$  etc., into two gamma-rays. Due to the isotropy of decay in the pion rest frame, the kinematics of this decay yields<sup>27</sup> a photon spectrum that is symmetric about  $m_\pi/2 \approx 67$  MeV, an unmistakable signature of the production of pions in astrophysical systems. Supernova remnant models of pion production and decay use some variant of a hybrid approach (e.g. see Dermer<sup>28</sup>), where low energy pion creation (for shock-accelerated proton momenta  $p_p$  below around 3 GeV/c) is mediated by an isobaric state  $\Delta(1232)$  (Stecker<sup>27</sup>), or a collection of different states, and the complexities of pion creation at high energies (for  $p_p \gtrsim 10$  GeV/c) is described by some adaptation<sup>29,30</sup> of Feynman scaling. Among the non-hadronic processes that are pertinent to SNR gamma-ray models is inverse Compton scattering by relativistic electrons<sup>31</sup>

of soft (i.e. low energy) photon fields such as the cosmic microwave background or infrared (IR) backgrounds local to the remnants. These contribute both X-rays and gamma-rays to the emission. At the same time, it is possible that electron synchrotron radiation, which can extend from radio up to X-ray energies, can act as seeds for the inverse Compton process. In addition, bremsstrahlung between relativistic  $e$  and ions and ISM electrons can generate gamma-rays, and form a potentially important part of gamma-ray models. Finally, Coulomb collisions, which are insignificant when the remnant environment is collisionless (for most of its lifetime), can help to redistribute electron and proton energies below 100 MeV when the remnant age exceeds  $10^4$  years<sup>32</sup>. These processes are addressed in one or other of the various papers discussed below.

### 3.1 The Two-Fluid Model of Drury et al.

The first gamma-ray emission model for supernova remnants presented in the recent wave of interest was the seminal work of Drury, Aharonian and Völk<sup>19</sup>, who computed the photon spectra and fluxes expected from the decay of neutral pions generated in collisions between shock-accelerated ions and cold ions in the ISM; they neglected the other electromagnetic processes mentioned just above. Their work used the *two-fluid* approach<sup>33,34</sup> to shock acceleration (discussed briefly in Baring<sup>20</sup>), treating the cosmic rays and thermal ions as separate entities (electrons go along for the ride). This technique explores the hydrodynamics of shocked flows taking into account these two components, obtaining solutions that conserve particle number, momentum and energy fluxes (per solid angle in their spherically symmetric application to SNRs); it therefore describes, in a fashion, non-linear effects<sup>20</sup> in shock acceleration. The two-fluid approach is extremely useful for time-dependent applications, and therefore is appropriate for SNRs, but generally contains little or no self-consistent spectral information (but see the recent work of Malkov and Völk<sup>35</sup>), in contrast to the Monte Carlo simulations discussed in Baring<sup>20</sup>. The model of Drury et al.<sup>19</sup> built on an earlier two-fluid analysis<sup>36</sup> of remnant evolution, which assumed particle diffusion in the Bohm limit<sup>20</sup> where diffusion mean free paths  $\lambda$  are comparable to the ion gyroradii  $r_g$ . They were able to map the gamma-ray luminosity and shock profile evolution, and determined that the luminosity peaked in the Sedov phase and was more or less constant throughout it. This is in accord with a maximal shock dissipation when the supernova ejecta is being compressed and significantly decelerated by the ISM.

Drury et al.<sup>19</sup> noted that their model required a high target density ( $> 100 \text{ cm}^{-3}$ ) to match the EGRET flux, a situation that seems inevitable if pion decay emission dominates gamma-ray spectral formation. They observed, furthermore, that the remnants should become limb-brightened with age, an effect that arises because the shock weakens with time so that the dominant gamma-ray flux is always “tied” somewhat to a region near the shock that is sampled by lower particle energies. This attachment naturally requires the ionic mean free path  $\lambda$  to be an increasing function of the momentum, so that particles of lower energies remain closer to the shock. While such a limb-brightening is seen in radio and X-ray images of remnants (e.g. Tycho and SN1006), higher angular resolution capability will be needed in gamma-ray telescopes before its existence, or otherwise, can be probed at high energies. Drury et al. noted that the flow profile modifications (see Figure 1) lead to a precursor width of about 1/10th of the shock radius. Despite its strengths, their work has two key spectral deficiencies. The first is that they are forced to *assume* a canonical test-particle power-law form for the ion populations, and hence do not describe self-consistently the intimate relationship (discussed below, and by Baring<sup>20</sup>) between non-linear modification of the flow profile and spectral curvature. Secondly, they assumed that the particles would be accelerated to at least 100 TeV and did not incorporate physical limits such as in Eq. (3) to the acceleration mechanism. This latter omission, promoted observational investigations by the Whipple collaboration that produced upper limits in the TeV energy range<sup>21</sup> that contradicted the Drury et al. predictions. While this conflict has been proposed as a failure for shock acceleration models of SNRs, realistic choices of  $E_{\text{max}}$  in Eq. (3)

actually yield model spectra that are quite compatible with the observational constraints.

### 3.2 More Recent Models

The next substantial development of models of gamma-ray emission from SNRs was the work of Gaisser, Protheroe and Stanev<sup>37</sup>. Their computation of emission fluxes and luminosities for bremsstrahlung, inverse Compton scattering, and decay of  $\pi^0$ s produced in hadronic collisions expanded beyond the consideration of Drury et al. However, they omitted consideration of non-linear shock dynamics in any form, did not treat time-dependence, and assumed just test-particle power-law distributions of protons and electrons, with arbitrary relative abundances (i.e.  $e/p$  ratios) in cosmic-ray populations. In their model, the inverse Compton scattering used both the microwave background and an infrared/optical background field local to the SNRs as seed soft photons. Their bremsstrahlung component was due to cosmic ray electrons colliding with ISM protons. The Gaisser et al. particle populations extended as power-laws beyond 30 TeV, with cutoffs only due to inverse Compton (IC) cooling, so that they included no treatment of spatial or temporal limits to acceleration. Consequently, they have exactly the same problem as Drury et al.<sup>19</sup> in that their model violates the TeV upper limits obtained by Whipple. At the same time the large hard X-ray synchrotron fluxes that would result from their model would violently conflict with observational limits. Gaisser et al. observed that, since the inverse Compton spectrum is intrinsically flatter than bremsstrahlung and pion decay spectra, this component needs to be suppressed to accommodate the EGRET spectral indices of the sources associated with  $\gamma$  Cygni and IC443. Hence they imposed a high matter density ( $> 300 \text{ cm}^{-3}$ ) to enhance bremsstrahlung and  $\pi^0$  decay to IC flux ratio. Such a goal can also be achieved, without resorting to extremely dense ambient media, by reducing the primary accelerated electron population. Note that  $\pi^\pm \rightarrow e^\pm$  secondaries are always unimportant for the SNR problem since the ion cooling time in pion production is much longer than typical remnant ages.

Very recently Sturmer, Skibo and Dermer<sup>32</sup> have developed a time-dependent model, where they use the Sedov solution in Eq. (1) for the expansion, and numerically solve time-dependent equations for electron and proton distributions subject to cooling by inverse Compton scattering, bremsstrahlung,  $\pi^0$  decay and synchrotron radiation. Essentially they have included all the radiation processes of Gaisser et al.<sup>37</sup>, and have added synchrotron emission to supply a radio flux. One variant on all previous work is their inclusion of Coulomb collisions, which they find can contribute to the cooling of non-thermal ions and electrons below 100 MeV for remnants older than  $10^4$  years. Like Gaisser et al., the work of Sturmer et al. is not really a shock acceleration model, but rather a time-dependent particle evolution and radiation emission approach. They assume canonical power-laws like Drury et al.<sup>19</sup> and Gaisser et al.<sup>37</sup>, and therefore have no handle on how non-linear shock modification effects determine the spectral index and curvature. They do not include any non-linear hydrodynamic effects as in Drury et al., and so omit any consideration of dynamic modifications to the Sedov solution. Sturmer et al. obtain gamma-ray emission that persists, as in Drury et al., into the radiative phase of remnant evolution. One feature of their model is the dominance of inverse Compton emission, which intrinsically has a flatter spectrum than either bremsstrahlung or pion decay radiation. This arises because they generally opt to have the same energy density in non-thermal electrons and protons, and therefore the shock-accelerated electrons are much more populous than their proton counterparts. The inappropriateness of this from the point of view of shock acceleration theory is discussed below. Sturmer et al.'s work possesses a significant advance over the previous work by introducing cutoffs in the distributions of the accelerated particles (actually first done by De Jager and Mastichiadis<sup>14,38</sup>), which are defined by the limits on the achievable energies in Fermi acceleration discussed above. Hence, given suitable model parameters, Sturmer et al. can accommodate the constraints imposed by Whipple's upper limits<sup>21</sup> to  $\gamma$  Cygni and IC 443.

## 4 Spectral Effects of Non-Linear Shock Acceleration

The models addressed so far have many assets, but also two noteworthy spectral limitations from the perspective of shock acceleration theory: (i) they do not pin down the steepness of, nor describe curvature in, the distribution of shock-accelerated ions and electrons, and therefore do not self-consistently determine the particle populations, and (ii) they possess no coherent prescription for the  $e/p$  ratio, an abundance ratio that is crucial to the formation of the gamma-ray spectrum. These deficiencies arise because their considerations of accelerated particle distributions are entirely test-particle in nature; Drury et al. used the two-fluid approach to analyze non-linear aspects of only the flow dynamics. A treatment of these non-linearities, which arise in supernova remnants because their shocks are strong so that the generated cosmic rays are endowed with a significant fraction of the total particle pressure, is essential for more accurate modelling of emission spectra. These spectral limitations are naturally remedied by the Monte Carlo simulational approach, as described in the accompanying review of Baring<sup>20</sup>. This kinematic technique can self-consistently model the feedback of the accelerated particles on the spatial profile of the flow velocity, which in turn determines the shape of the particle distribution. To re-cap the discussion in Baring<sup>20</sup>, the accelerated population pushes on the upstream plasma and decelerates it before the discontinuity is reached, so that an upstream *precursor* forms, in which the flow speed is monotonically decreasing. At the same time, the cosmic rays press on the downstream gas, slowing it down too. The overall effect is one where the total compression ratio  $r$ , from far upstream to far downstream of the discontinuity, actually **exceeds that of the test-particle scenario**. This situation, which results from the need of the flow to increase  $r$  to adjust for energy and momentum escape<sup>39,40</sup>, is illustrated in the left hand panel of Figure 2, where the flow profile is depicted in the rest frame of the shock: notice the inversion from the observer's perspective of the profile that is depicted in Figure 1.

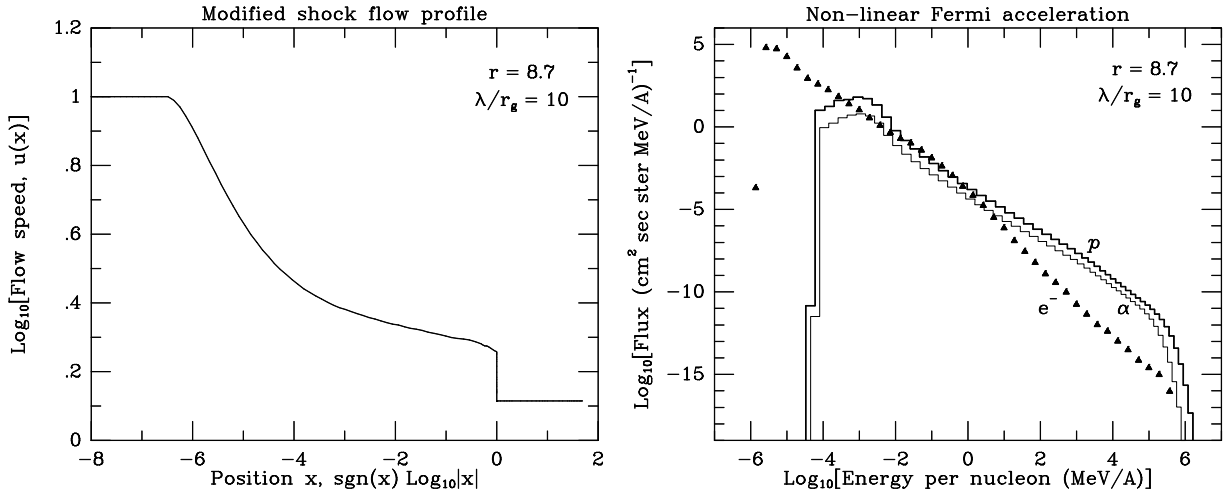


Figure 2: The velocity profile of fluid flow for a Monte Carlo simulation of a non-linear shock that is modified by the cosmic ray pressure is depicted on the left. The abscissa represents the position  $x$  relative to the shock ( $> 0$  downstream) in units of the mean free path of particles with speed  $u_1$ . Mostly the abscissa is defined by the logarithmic form  $\text{sgn}x \log_{10}|x|$ , but it is linear in  $x$  for a small range near the shock. On the right are the particle distributions (protons: heavy histogram,  $\text{He}^{2+}$ : light histogram, electrons: triangles) obtained by the simulation run that generated the profile on the left. In this instance, a compression ratio of  $r = 8.7$  resulted.

Typical distributions of particles that are accelerated in *modified shock* flow profiles like that of Figure 2 are presented in numerous papers<sup>39,40,41,42</sup>: these resemble the right hand panel of Figure 2, which is the distribution that was obtained self-consistently<sup>44</sup> by the Monte Carlo simulation technique in conjunction with the profile in the left hand panel. The maximum energies in these distributions were determined via the spatial constraint that leads to Eq. (3).

Figure 2 therefore embodies the intimate relationship between non-linear modification of the flow profile and *upward* spectral curvature that is the trademark<sup>39,40</sup> of non-linear acceleration. Such curvature is a consequence of the use of a momentum-dependent mean free path  $\lambda$  in the Monte Carlo model. When  $\lambda$  is an increasing function of momentum, an assumption that is supported by inferences of particle diffusion from the Earth's bow shock and also in hybrid plasma shock simulations<sup>43</sup>, the higher energy particles sample large scales in their diffusion in the shock environs. Hence they experience a greater effective compression ratio (see Figure 2), and consequently yield a flatter spectral index than at low energies. This curvature is important for gamma-ray emission models, since it introduces enhancements in the TeV range by factors of 2–3 relative to the EGRET range; such increases can be the difference between detection and non-detection by air Čerenkov experiments like Whipple, MILAGRO and CAT.

Gamma-ray emission spectra that are generated by the self-consistent Monte Carlo approach to shock acceleration are depicted in Baring, Ellison and Grenier<sup>45</sup> and Baring et al.<sup>44</sup>. The former work focuses on just neutral pion decay emission, while the latter also includes bremsstrahlung, synchrotron and inverse Compton emission components for SNRs. In both papers, the cessation of acceleration above critical energies in the 1 TeV - 10 TeV range caused by the spatial and temporal limitations of the expanding SNR shell [i.e. according to Eq. (3)] yields gamma-ray spectral cutoffs, so that the resulting emission spectra appear to be consistent with Whipple's TeV upper limits<sup>21</sup> to those EGRET's unidentified sources that have SNR associations. Hence, as in Sturmer et al.<sup>32</sup>, the Whipple upper limits pose no serious problem, but rather now provide powerful diagnostic constraints to our theoretical understanding. For example, combining Eqs. (1) and (3), the value of  $E_{\max}$  is quite insensitive (in the Sedov phase) to the SNR age so that sufficiently low values of  $E_{\max}$  can only be obtained for low field strengths  $B_1$  or supernova energies  $E_{\text{SN}}$ . This requirement can be quite stringent if non-thermal X-ray emission also constrains the field strength, as will be discussed below. Note that  $E_{\max}$  always peaks early in the Sedov phase. The cosmic ray spectral curvature plays a vital role in determining the emission fluxes as the spectrum rolls over just below the cutoff, an important consideration for possible detections by future instrumentation such as GLAST, VERITAS and Celeste. Note that the Monte Carlo approach of Baring et al.<sup>44,45</sup> is not time-dependent, a limitation that may not be serious at all, given that the upstream precursor scalelength of  $\sim 0.1r_{\text{sk}}$  that was obtained by Drury et al.<sup>19</sup> was used as simulational input for the scale on which particles escape the shock. On this scale, the effects of shock curvature can be neglected.

Another prominent feature of the distributions in Figure 2 is the low value of the electron to proton ratio above 1 GeV. This strongly contrasts the situation of Sturmer et al.<sup>32</sup>, who have an electron-dominated cosmic ray component. The reason the Monte Carlo simulations produce a minority of non-thermal electrons (even though the thermal populations satisfy charge neutrality) is that both proton and electrons are injected directly from thermal energies. The electrons, however, suffer from a suppression of injection due to a potential absence of resonant waves<sup>20</sup> to effect diffusion until they reach around 1 MeV. This property of plasmas is modelled by Baring et al.<sup>44</sup> via an electron mean free path that exceeds that of protons at energies below around 1 MeV. For non-relativistic particle speeds, electrons have shorter  $\lambda$  than do protons of comparable kinetic energies, and hence sample smaller compressions in the modified shock profile. The net result is that the electron distribution is steep enough at low energies so as to render the  $e/p$  ratio much less than unity above 1 GeV. This determination is entirely consistent with the observation that electrons supply around 2% of the cosmic ray population by number (e.g. Müller et al.<sup>46</sup>), and also blends with limits on the local  $e/p$  abundance ratio imposed when modelling the galactic gamma-ray background<sup>47</sup>. The values of  $e/p$  much greater than unity in the Sturmer et al.<sup>32</sup> model grossly violate these observations and the understanding of wave properties in plasmas just mentioned. Future measurements of the unidentified sources by more sensitive experiments in the 1–100 MeV range should constrain the  $e/p$  ratio.



## 5 A Myriad of Possibilities

While the focus here has been on gamma-rays from remnants, much can be learned from studying other wavebands also. This has been the approach of Mastichiadis and De Jager<sup>38,14</sup>, who have examined the remnants SN1006 and W44. For SN1006, which has not been seen in gamma-rays, they used<sup>38</sup> the recent observations<sup>8</sup> of non-thermal X-rays by ASCA to constrain the energy of electrons and the magnetic field, interpreting the X-ray flux as being of synchrotron origin. This contention (see also Reynolds<sup>9</sup>) assumes that the steep X-ray spectrum is part of a rollover in the electron distribution at energies around 100 TeV. Using microwave and infrared backgrounds appropriate to SN1006, Mastichiadis and De Jager<sup>38</sup> predicted the resulting inverse Compton component in gamma-rays, and determined that it would always satisfy the EGRET upper bounds. However, they concluded that TeV upper limits from experiments like Whipple could potentially constrain the parameter  $\eta = \lambda/r_g$  in Eqs. (2) and (3) to values signifying departure from Bohm diffusion (i.e.  $\eta \gg 1$ ), otherwise the TeV flux would exceed that of the Crab nebula. Pinning the X-ray synchrotron spectrum determines  $E_{\text{max}}^2 B$  and also a combination of  $B$  and the electron density. From Eq. (3),  $\eta$  therefore couples to  $B$  and the gamma-ray inverse Compton flux must anti-correlate with both  $B$  and  $\eta = \lambda/r_g$ .

At the same time, De Jager and Mastichiadis<sup>14</sup> have proposed that the radio spectrum in W44 is too flat to be explained by a shock-accelerated electron population. This is not necessarily the case, given the flat distributions (i.e. flatter than  $E^{-2}$ ) that can be attained at relativistic energies (see Figure 2), however they have conjectured that the pulsar that is present in W44 may inject electrons with the required distribution via its relativistic wind, thereby circumventing the need to invoke Fermi acceleration at the remnant's shock. This opens up the possibility that plerionic sources are distinct in their acceleration properties from non-plerionic ones, despite displaying similar emission properties: W44 is a good candidate for the unidentified EGRET source 2EG J1857+0118. Add to this the fact that the Vela pulsar has a wind nebula but no observable gamma-ray emission associated with the outer extremity (i.e. shell) of its remnant, and the picture is confused further. De Jager and Mastichiadis<sup>14</sup> suggest that inverse Compton emission and bremsstrahlung dominate the gamma-rays in W44, and invoke a high  $e/p$  ratio; the EGRET data and Whipple upper limits can still accommodate a pion decay origin for gamma-rays and low  $e/p$  ratios without compromising the radio continuum.

These papers serve to underline the diversity of the handful of remnants that are associated with EGRET unidentified sources. Such a diversity is also reflected in their morphological properties, their optical/IR spectra and line emission, environmental densities, etc., and also the role of pulsars and plerionic contributions. In short, these remnants must be considered on a case-by-case basis. Yet all have proximity to dense molecular clouds of various sorts, providing a strong clue to the reason for gamma-ray emission: a consensus that the presence of dense molecular clouds may be the driving force and signature of gamma-ray bright remnants seems to be emerging. By the same token, the gamma-ray emitters must be a minority of remnants (perhaps mostly young) given that they cannot produce ions above around a few TeV in profusion: remnants that provide cosmic rays up to the knee must be a gamma-ray quiet majority. Much remains to be explored in this field, in particular the relationship between the clouds and the shock parameters, the degree of ionization of the environment, the precise location of the gamma-ray emission, differentiation between plerion-driven and shock-powered gamma-ray sources, and the maximum energies and relative abundances of the produced cosmic rays. The Whipple upper limits have not destroyed the hypothesis that SNR shocks energize the particles responsible for the gamma-ray emission, but rather are a blessing in disguise, providing a powerful tool for constraining models. The next generation of gamma-ray telescopes, with better angular resolution and cumulatively-broad spectral range will have a significant impact on this field, particularly in coordination with X-ray and radio observations.

**Acknowledgments:** I thank my collaborators Steve Reynolds, Isabelle Grenier and Don Ellison, and also Okkie De Jager for many informative discussions about supernova remnants and shock acceleration theory. I also thank Joe Esposito for providing the images used in Figure 1.

## References

1. Lagage, P. O. & Cesarsky, C. J. *Astron. Astrophys.* **125**, 249 (1983).
2. Hillas, A. M. *Ann. Rev. Astron. Astrophys.* **22**, 425 (1984).
3. Blandford, R. D. & Eichler, D. *Phys. Reports* **154**, 1 (1987).
4. Green, D., SNR catalogue on the WWW at <http://www.mrao.cam.ac.uk/surveys/snrns/>
5. Borkowski, K. J. et al. *Astrophys. J.* **466**, 866 (1996).
6. Ellison, D. C. et al. *Pub. Astron. Soc. Pacific* **106**, 780 (1994).
7. Keohane, J. W., Rudnick, L. & Anderson, M. A. *Astrophys. J.* **466**, 309 (1996).
8. Koyama, K. et al. *Nature* **378**, 255 (1995).
9. Reynolds, S. P. *Astrophys. J. Lett.* **459**, L13 (1996).
10. Keohane, J. W., et al. *BAAS* **188**, 74.02 (1996).
11. Allen, G. E. et al. *BAAS* **189**, 55.06 (1996).
12. Esposito, J. A., Hunter, S., Kanbach, G. & Sreekumar, P. *Astrophys. J.* **461**, 820 (1996).
13. Sturmer, S. J. & Dermer, C. D. *Astron. Astrophys.* **293**, L17 (1995).
14. De Jager, O. C. & Mastichiadis, A. *Astrophys. J.* in press.
15. Thompson, D. J. et al. *Astrophys. J.* **436**, 229 (1994).
16. Kaaret, P. & Cottam, J. *Astrophys. J. Lett.* **462**, L35 (1996).
17. Higdon, J. C. & Lingenfelter, R. E. *Astrophys. J. Lett.* **198**, L17 (1975).
18. Chevalier, R. A. *Astrophys. J.* **213**, 52 (1977).
19. Drury, L. O'C., Aharonian, F. A. & Völk, H. J. *Astron. Astrophys.* **287**, 959 (1994).
20. Baring, M. G., review paper on shock acceleration in this volume.
21. Lessard, R. W., et al. *Proc. 24th ICRC (Rome)* **II**, 475 (1995).
22. Lang, K. R. *Astrophysical Formulae*, (Springer-Verlag, Berlin, 1980).
23. Forman, M. A., & Morfill, G. *Proc. 16th ICRC (Kyoto)* **V**, 328 (1979).
24. Jokipii, J. R. *Astrophys. J.* **313**, 842 (1987).
25. Ellison, D. C. Baring, M. G., & Jones, F. C. *Astrophys. J.* **453**, 873 (1995).
26. Drury, L. O'C., Duffy, P. & Kirk, J. G. *Astron. Astrophys.* **309**, 1002 (1996).
27. Stecker, F. W. *Cosmic Gamma Rays*, (NASA SP-249, NASA, Washington, 1971)
28. Dermer, C. D. *Astron. Astrophys.* **157**, 223 (1986).
29. Stephens, B. A., & Badhwar, G. D. *Astrophys. Sp. Sci.* **76**, 213 (1981).
30. Tan, L. C. & Ng, L. K. *J. Phys. G. Nucl. Phys.* **9**, 1289 (1983).
31. Rybicki, G. & Lightman, A. *Radiative Processes in Astrophysics* (Wiley, New York, 1979)
32. Sturmer, S. J., Skibo, J. G., & Dermer, C. D. *Astrophys. J.*, submitted.
33. Drury, L. O'C., & Völk, H. J. *Astrophys. J.* **248**, 344 (1981).
34. Drury, L. O'C. *Rep. Prog. Phys.* **46**, 973 (1983).
35. Malkov, M. A. & Völk, H. J. *Astron. Astrophys.* **300**, 605 (1995).
36. Drury, L. O'C., Markiewicz, W. J. & Völk, H. J. *Astron. Astrophys.* **225**, 179 (1989).
37. Gaisser, T. K., Protheroe, R. J. & Stanev, T. *Astrophys. J.*, submitted.
38. Mastichiadis, A. & De Jager, O. C. *Astron. Astrophys.* **311**, L5 (1996).
39. Eichler, D. *Astrophys. J.* **277**, 429 (1984).
40. Ellison, D. C., & Eichler, D. *Astrophys. J.* **286**, 691 (1984).
41. Jones, F. C. & Ellison, D. C. *Space Sci. Rev.* **58**, 259 (1991).
42. Ellison, D. C. Baring, M. G., & Jones, F. C. *Astrophys. J.* **473**, 1029 (1996).
43. Giacalone, J., Burgess, D., Schwartz, S. & Ellison, D. *Astrophys. J.* **402**, 550 (1993).
44. Baring, M. G., Ellison, D. C., Reynolds, S. P., Grenier, I. & Goret, P., in preparation.
45. Baring, M. G., Ellison, D. & Grenier, I., in *Proc. 2nd Integral Workshop*, (ESA, in press).
46. Müller, D., et al. *Proc. 24th ICRC (Rome)* **III**, 13 (1995).
47. Hunter, S. D., et al. *Astrophys. J.*, in press (May 20, 1997).